Seasonal and interannual variability of climate and vegetation indices across the Amazon

Paulo M. Brando[a,b,c,1], Scott J. Goetz[c], Alessandro Baccini[c], Daniel C. Nepstad[c], Pieter S. A. Beck[c], and Mary C. Christman[d]

[a]Instituto de Pesquisa Ambiental da Amazônia, 66035-170 Belém, Brazil; [b]Department of Biology and School of Natural Resources and Environment and [d]Department of Statistics and Institute of Food and Agricultural Sciences, University of Florida, Gainesville, FL 32611; and [c]Woods Hole Research Center, Falmouth, MA 02450

Edited* by Ruth S. DeFries, Columbia University, New York, NY, and approved July 13, 2010 (received for review August 3, 2009)

Drought exerts a strong influence on tropical forest metabolism, carbon stocks, and ultimately the flux of carbon to the atmosphere. Satellite-based studies have suggested that Amazon forests green up during droughts because of increased sunlight, whereas field studies have reported increased tree mortality during severe droughts. In an effort to reconcile these apparently conflicting findings, we conducted an analysis of climate data, field measurements, and improved satellite-based measures of forest photosynthetic activity. Wet-season precipitation and plant-available water (PAW) decreased over the Amazon Basin from 1996–2005, and photosynthetically active radiation (PAR) and air dryness (expressed as vapor pressure deficit, VPD) increased from 2002–2005. Using improved enhanced vegetation index (EVI) measurements (2000–2008), we show that gross primary productivity (expressed as EVI) declined with VPD and PAW in regions of sparse canopy cover across a wide range of environments for each year of the study. In densely forested areas, no climatic variable adequately explained the Basin-wide interannual variability of EVI. Based on a site-specific study, we show that monthly EVI was relatively insensitive to leaf area index (LAI) but correlated positively with leaf flushing and PAR measured in the field. These findings suggest that production of new leaves, even when unaccompanied by associated changes in LAI, could play an important role in Basin-wide interannual EVI variability. Because EVI variability was greatest in regions of lower PAW, we hypothesize that drought could increase EVI by synchronizing leaf flushing via its effects on leaf bud development.

drought | enhanced vegetation index | moderate-resolution imaging spectroradiometer | tropical | carbon cycling

The accumulation of heat-trapping gases in the atmosphere may subject large areas of the Amazon Basin and other tropical forest formations to more frequent and severe drought in the coming decades (1). This trend may interact synergistically with regional inhibition of rainfall driven by deforestation (2–4) and more frequent sea-surface temperature anomalies (5–7) to move these tropical forest regions toward forest dieback events. Drier and warmer climate in the region favors the persistence of grasses and shrubs over trees in a process that is reinforced by recurring fire (8).

It is difficult to assess the drought thresholds beyond which forest dieback might occur, in part because of conflicting evidence regarding the response of forest photosynthesis to drought (9–13). Some studies suggest that forest photosynthesis (gross primary productivity, GPP) increases during the early stages of drought because of higher photosynthetically active radiation (PAR) (14–16). In contrast, two partial throughfall exclusion experiments conducted in the Amazon region found proxies of forest productivity all declined under mild drought conditions, with tree mortality increasing under high cumulative canopy water stress resulting from limited plant-available water (PAW) (reviewed in ref. 17). These impacts were observed only after 2–3 y of simulated drought, with the lag probably resulting from plant adaptations to reduced availability of soil water (18).

These apparently contradictory findings were particularly striking in 2005, when the most severe drought of the last 100 y affected the southwestern Amazon (7). This dry and warm period, linked to an anomalously warm tropical North Atlantic, provided an opportunity to evaluate forest resistance to drought over a greater spatial extent than the partial throughfall experiments noted above. Two studies reporting on this drought event diverged in their findings. Phillips et al. (19) found evidence that intact forests of the Amazon Basin were drought-sensitive, accumulating 1.2–1.6 Pg less carbon during the drought period of 2004–2005 than in previous years, and concluded that Amazonian forests were negatively affected by the drought of 2005. Conversely, Saleska et al. (20) found that intact Amazon forests experiencing anomalously low precipitation (PPT) in 2005 had higher photosynthetic activity, as indicated by the enhanced vegetation index (EVI), a canopy reflectance metric developed to minimize the attenuating influences of background and atmospheric effects and thus remain effective even in areas of high biomass and chlorophyll content (21). The authors of the latter study concluded that these forests were more drought resistant than previously thought. A possible resolution of this conflict was provided by a recent paper by Samanta et al. (22) that suggested that the higher EVI observed in 2005 (20) could be attributable to atmospherically induced variations associated with aerosol loadings.

We conducted a study to understand better the responses of tropical forests to climate extremes, particularly the processes that permit forests to sequester carbon during drought conditions. First, we evaluated the temporal patterns of climatological variables from 280 meteorological stations (1996–2005), PAR from the Geostationary Operational Environmental Satellite (GOES), and an improved EVI dataset (*Methods*) from the Moderate Resolution Imaging Spectroradiometer (MODIS) over the dry seasons of 2000–2008 across the Amazon Basin. Second, we examined statistical relationships between EVI during the dry season (July–September) and three integrative climate variables [vapor pressure deficit (VPD), PPT, and modeled PAR]. We analyzed the EVI–climate variable relationships for both the entire Amazon Basin (intraannually) and for the densely forested areas only (interannually). For the Basin-wide analysis, we predicted that EVI within a given year would become more sensitive to drier climatic conditions (e.g., high VPD and low PPT) across a gradient of percentages of canopy cover. In densely forested areas (≥70% canopy cover; *Methods*), we predicted that interannual EVI variability would be correlated positively with modeled PAR in sites with high precipitation history (i.e., average

Author contributions: P.M.B., S.J.G., and D.C.N. designed research; P.M.B., S.J.G., A.B., and P.S.A.B. performed research; P.M.B., A.B., P.S.A.B., and M.C.C. analyzed data; and P.M.B., S.J.G., and D.C.N. wrote the paper

The authors declare no conflict of interest.

*This Direct Submission article had a prearranged editor.

Freely available online through the PNAS open access option.

[1]To whom correspondence should be addressed. E-mail: pmbrando@ipam.org.br.

This article contains supporting information online at www.pnas.org/lookup/suppl/doi:10.1073/pnas.0908741107/-/DCSupplemental.

monthly dry-season precipitation for 1996–2005 >100 mm). We also predicted that EVI would be negatively correlated with VPD in locations with low PPT history (<100 mm per dry-season month), where dry-season VPD is likely to limit productivity, thus reducing leaf production and leaf area. Finally, using data at relatively high spatial (0.25 km^2) and temporal resolution, we evaluated the EVI relationships not only on the basis of these climate variables but also with monthly field measurements of leaf area index (LAI), litterfall, and new leaf production in a dense forest near Santarem, Brazil.

Results

Spatial–Temporal Patterns of EVI. EVI varied spatially and temporally across the Amazon Basin during 2000–2008 (Fig. 1). Generally, EVI varied most where soil moisture availability (PAW) was most variable. There was a strong gradient in mean annual EVI from the western to the central portion of the Basin, with associated gradients in the variability of EVI and in the estimated average annual PAW from depths of 0–10 m.

In areas with a high percentage (>70%) of fractional canopy cover (hereafter simply "canopy cover"), roughly defining the area of intact forest across the Basin (Fig. 2), EVI was below average in 2000, 2001, 2004, and 2007, close to average in 2003 and 2008, and above average in 2005 and 2006 (Fig. S1). Pronounced shifts in the annual anomalies (deviations from 2000–2008 mean values) were observed over short time periods. For example, anomalies in 2002 were 151% higher than in 2001; in 2005 they were 168% higher than in 2004; and in 2007 they were 257% lower than 2006. Analysis of the spatial covariation of EVI and PAW revealed that interannual EVI variability in dense forests was slightly higher in drier areas, with EVI variability decreasing gradually as average PAW increased (Fig. 1 and Fig. S2).

Basin-Wide Climate. The Amazon Basin experienced a decline in annual rainfall and an increase in PAR from 1996–2005. Based on data from ~280 meteorological stations distributed across the Amazon (Fig. 1), we found that annual wet-season PPT decreased at a rate of 5.31 ± 0.68 mm y^{-1} (Fig. 3 and Table 1). Dry-season PPT also tended to decrease over this time period, but not significantly (Table 1). In contrast, PAR increased over the period 1996–2005, primarily after 2002 (especially during the wet season), but the rate was statistically significant only for the dry season (12.22 ± 4.51 moles m^{-2} $month^{-1}$ y^{-1}). There was not a strong temporal trend in VPD over the entire time period, but VPD increased substantially after 2002 (Fig. 3). For example, although the rate of increase of average VPD during 1996–2000 was modest (0.0029 kPa y^{-1}), it increased to 0.43 kPa y^{-1} during 2002–2005. As a result of decreased PPT and increased VPD, modeled PAW from 0–10 m depth decreased significantly over the time period at a rate of 2.03 ± 0.22% during the wet season and 2.21 ± 0.11% y^{-1} during the dry season (similar climatic patterns were observed for areas of high canopy cover; Table 1).

EVI and Climate Variables. ***Spatial analysis across the Amazon basin.*** In areas with mixtures of vegetation types (e.g., pastures, cerrado, and secondary and primary forests), we predicted that EVI would decrease with (*i*) increasing VPD and (*ii*) decreasing PPT and percentage of canopy cover. Spatial analysis of EVI data from 256 cells (64 km^2) surrounding each meteorological station generally supported our predictions. There was a strong and significant relationship between canopy cover and VPD in 4 of the 6 y of the study (Table S1). Thus, EVI tended to decrease as VPD increased in areas of low canopy cover. Similarly, PPT was related to canopy cover in 3 of 6 y in the study, but only marginally ($P <$ 0.1); as PPT decreased in areas of sparse canopy cover, EVI also decreased. In contrast, PAR showed a marginally significant relationship with canopy cover in only 1 y ($P = 0.054$). Thus only in 2004 did EVI increase as PAR increased in areas with a high percentage of canopy cover. In addition to general linear models, we used hierarchical partitioning (23) to estimate the relative influence of each predictor on EVI, accounting for collinearity among predictors in a linear model (*Methods*). Based on this analysis, canopy cover, VPD, and latitude explained, respectively, 55%, 17%, and 11% of the total variation associated with the full model (average R^2 of the full model, *M1*: ~56%) (*Methods*).

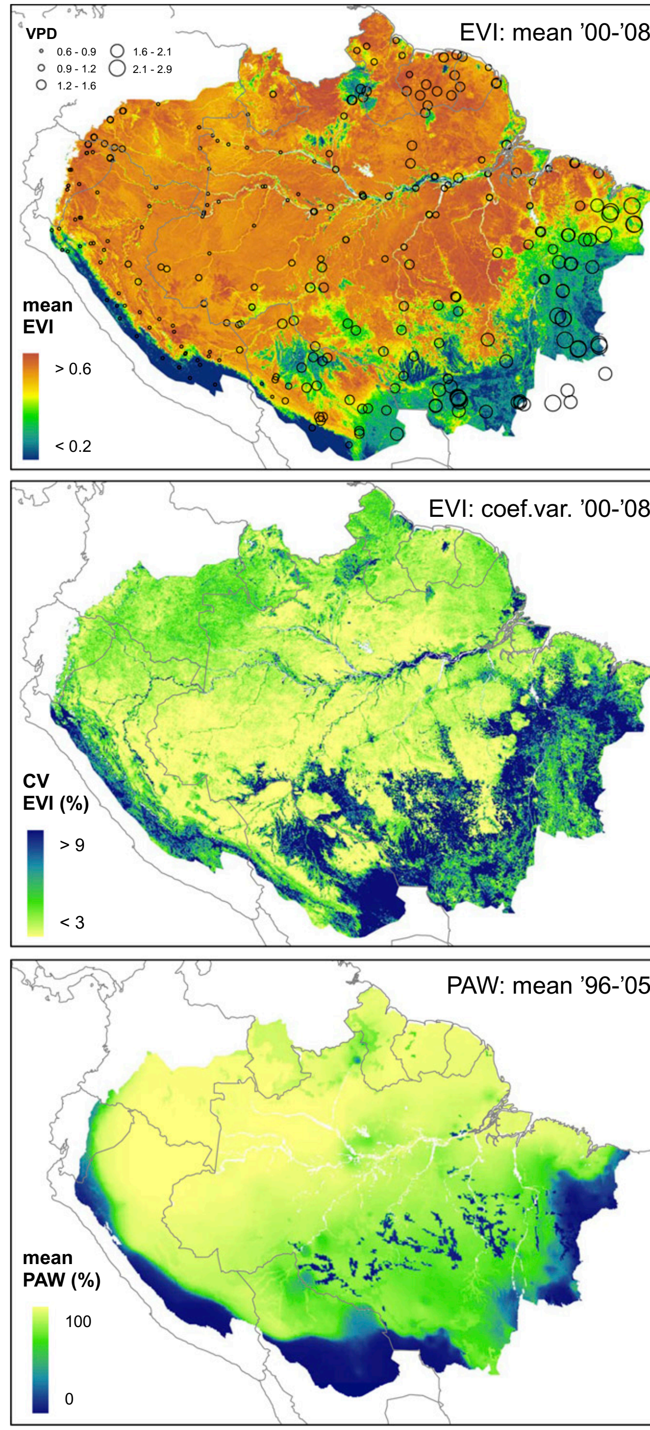

Fig. 1. (*Top*) Average dry-season EVI across central South America for the period 2000–2008. Overlaid circles represent average VPD measured at 280 meteorological stations across the region for the period 1996–2005. (*Middle*) Coefficient of variation in annual EVI for the period 2000–2008. (*Bottom*) Average annual PAW at 10-m depth, expressed as a percentages of the maximum, for the period 1996–2005. Note that the scale here is amplified relative to Fig. 2.

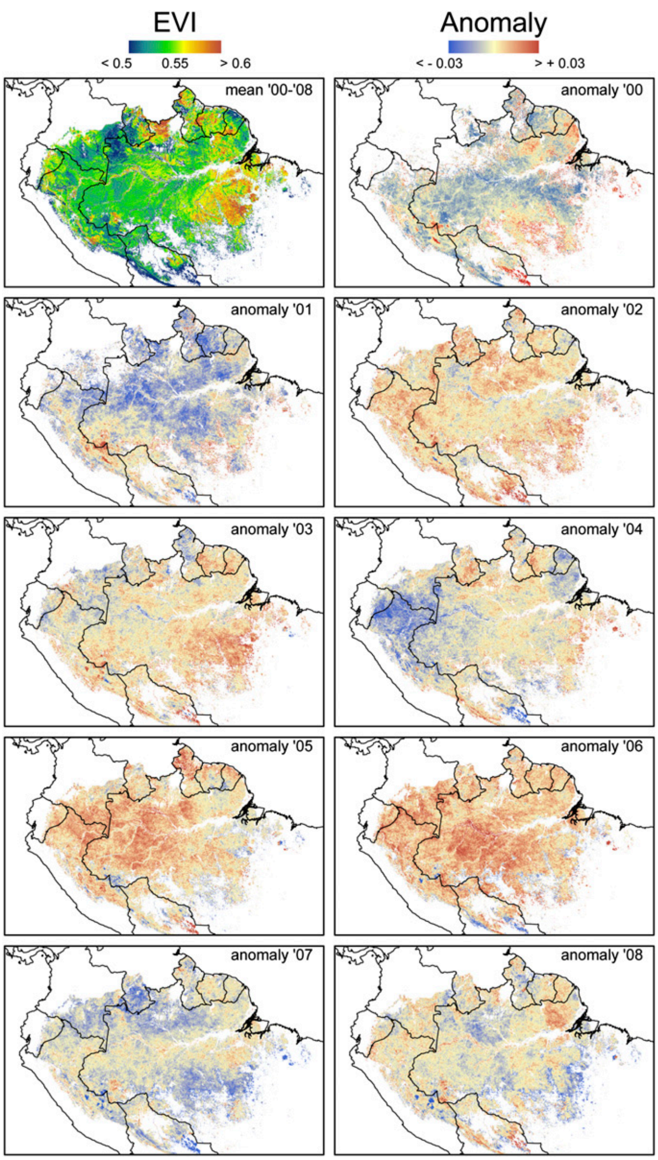

Fig. 2. Spatial–temporal patterns of dry-season EVI across the Amazon for areas with high percentage of canopy cover (EVI >0.4 and MODIS canopy cover product >70%). The panel at the top left shows average EVI from 2000–2008 (referred in the figure as '00-'08). Other panels show the EVI anomaly, calculated as $EVI_i - EVI_{mean}$, for each year, as indicated.

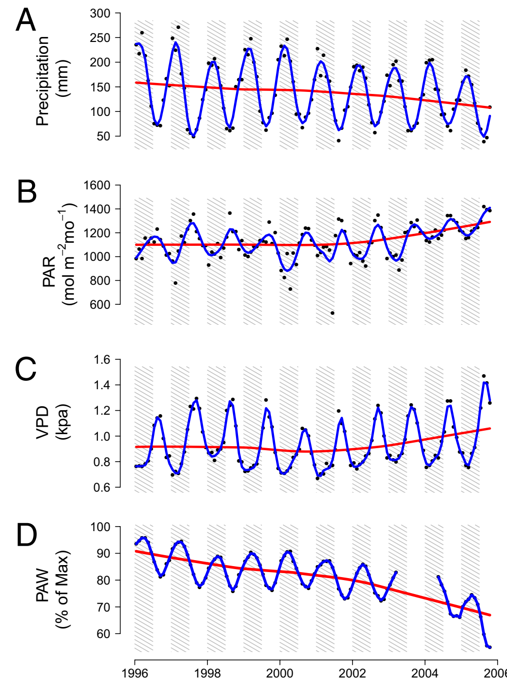

Fig. 3. Monthly climate patterns over the Amazon region based on data from 280 meteorological stations distributed across the basin. (*A*) Monthly averages of precipitation. (*B*) Monthly modeled PAR. (*C*) Modeled monthly PAW at 10-m depth. (*D*) Monthly VPD. Blue lines represent a smooth curve based on a loess method, and red lines represent a local regression model (spline).

Overall, these results indicate a moderately strong effect of VPD and a weaker effect of PPT and PAR on EVI from 2000–2005 (note that the quality of PAR data may account in part for the weak association between EVI and PAR; *Methods*). These results also suggest that spatial gradients, independent of variations in climate, had important effects on EVI.

Spatial–temporal analysis in densely forested areas. In densely forested areas (i.e., all cells with ≥70% canopy cover), there was no support for the hypothesis that interannual EVI variability was associated with temporal variation in PAR, VPD, or PPT across all classes of PPT history (Table S2). Rather, the only significant predictors of EVI were longitude ($P = 0.02$) and PPT history alone ($P = 0.108$) (Table S2). Using hierarchical partitioning analysis to assess the importance of each predictor of a linear model on EVI, *M2* (*Methods*), we found that spatial gradients accounted for most of the EVI variability. For example, of the 77% of the variation explained by the linear model, spatial variability alone accounted for 91% of this variation, whereas year, VPD, and PAR accounted for only 4.2%, 0.5%, 0.45%, respectively. Overall, these results show that no climatic variable could meaningfully explain the EVI interannual variability. This finding also was true when considering the effects of temporal autocorrelation and spatial gradients, the latter of which is influenced by the selection of months representing the dry season (*Methods*).

Site-Specific Analysis. At the intensively studied Tapajos site (near Santarem; 80% canopy cover), we found that monthly EVI was highly seasonal and thus positively and strongly correlated with field measurements of the proportion of trees (≥10 cm in diameter at breast height) with new leaves ($R^2 = 44\%$; $P < 0.01$). EVI also correlated positively with field measurements of PAR ($R^2 = 37\%$; $P < 0.01$) but correlated inversely with PAW from 0–2 m depth ($R^2 = 40\%$; $P < 0.01$), indicating there were no soil water constraints on photosynthesis (as 0–2 m PAW decreased, EVI increased) (Fig. 4 and Fig. S3). Hence, EVI was most sensitive to production of new leaves and associated light levels (the individual effects of PAR and leaf phenology on EVI could not be decoupled in our analysis). This interpretation is reinforced by our finding that field-measured LAI varied little between seasons and was poorly correlated with EVI ($R^2 = 10\%$; $P = 0.07$) and that EVI varied with dry-season litterfall (Fig. S3). Although other environmental variables also may have affected EVI indirectly (for example, via lagged effects on vegetation processes), their direct relationships with EVI were not evident.

In contrast to EVI derived from the MODIS-corrected reflectance products (*Methods*), the MODIS "standard collection 5 product" screened using standard-quality control flags (22) was poorly correlated with these measured seasonal environmental and biophysical variables (Fig. S4). These results indicate that the EVI product used for our analyses (produced from bidirectionally corrected reflectance data sets) was more sensitive to field conditions than the standard MODIS EVI product. This

Table 1. Slopes of precipitation, PAR, and VPD over time

	Meteorological stations surrounded by *all* fractions of forest cover		Meteorological stations surrounded only by *high* fraction of forest cover	
	Wet season	Dry season	Wet season	Dry season
Precipitation (mm)	−5.31 ± 0.68***	−0.35 ± 0.91	−7.79 ± 1.62***	−1.35 ± 1.13
PAR (moles m^{-2} mo^{-1})	10.38 ± 7.64	12.22 ± 4.51**	12.44 ± 8.21	11.23 ± 4.45**
VPD (kPa)	0.00 ± 0.00	0.00 ± 0.01	0.00 ± 0.00	0.00 ± 0.00
PAW (% of maximum)	−2.03 ± 0.22***	−2.21 ± 0.11***	—	—

All linear models between these climatic variables and time were fit using a linear mixed model with random effects of space and time, except for PAW. PAW was averaged over space and regressed over time (**$P < 0.05$; ***$P < 0.001$).

improvement could be a result of correction of viewing-angle conditions, screening procedures for cloud cover, or both. Although we cannot ensure the results at the Tapajos sites extend across the entire Amazon Basin, particularly because this site was not affected by severe drought during the study period, confidence in our regional results was supported by these more local-scale observations.

Discussion

Increases in solar radiation during dry periods may boost tropical forest productivity (14, 15, 24), but prolonged and severe droughts ultimately limit this effect by inducing stomatal closure and even tree mortality (25, 26). The thresholds at which drought starts to reduce productivity (as opposed to increasing it) still are not well known. Although satellite-based vegetation indices allow insight into potential environmental thresholds (27–29), they have provided conflicting indications of vegetation responses to drought in the Amazon Basin. Here we demonstrate that spatial variations of an improved EVI metric, corrected for bidirectional reflectance variations and other potential attenuating influences (30), were associated with gradients of PAW and VPD. This association indicates that EVI captured complex spatial patterns of photosynthetic responses to environmental variables across the Basin. In particular, we show contrasting responses of EVI to the relationship between tree canopy cover and drought over a wide range of environments (e.g., pasture, secondary forest, cerrado). These results reinforce findings from previous studies that demonstrated that where the percentage of tree canopy cover is high, trees are better buffered against drought because of their deep root systems (31, 32). Further, these results indicate that this buffering mechanism may not be restricted to the central Amazon (28).

In Tapajos's dense forest, even subtle changes in EVI captured complex seasonal ecosystem dynamics. In particular, the EVI corrected for bidirectional reflectance variations (*Methods*) increased with the number of canopy trees with new leaves, whereas the LAI varied little between seasons. These findings strongly suggest that seasonal variation in leaf flushing and PAR were associated with variations in EVI and therefore GPP (33). The association between EVI and PAR was more apparent at the seasonal timescale in the Tapajos forest ($R^2 = 35\%$) than in our Basin-wide analysis of densely forested areas in which interannual EVI generally was not responsive to any specific climatic variable. This finding raises the possibility that mechanisms other than PAR could be driving the EVI interannual variability. We propose three possible mechanisms for this observation.

First, given the strong correlation between EVI and the number of trees with new leaves observed at Tapajos, it is reasonable to expect that leaf flushing could have played a role in the Basin-wide interannual variability in EVI. Although leaf flushing usually coincides with periods of increased radiation (34), leaf bud break is cued not by radiation but by gradual changes in day length (35). Once bud break occurs, however, leaf development is controlled by water availability for cell expansion. Therefore, changes in tree water status modified by precipitation events (or even by leaf shedding) during the dry season of dry years is likely to synchronize bud development and, consequently, leaf flushing. Because we show that interannual EVI variability in dense forests during the dry season was greatest in regions of lower PAW, we hypothesize that drought could increase EVI by synchronizing leaf flushing via its effects on leaf bud development and tree water status. This hypothesis could explain, in part, the high anomalies during dry years (e.g., 2005). During wetter years (i.e., 2000 and 2001), leaf production would be less synchronous than in drier years, resulting in a lower number of pixels with highest EVI observed during the period from July–September. We suggest that this phenomenon is a potentially important area of research.

Second, the lack of a relationship between PAR and Basin-wide EVI could be associated with long-term adaption for herbivory avoidance. It has been suggested that the timing of leaf flushing of tropical trees is the result of selective processes to coincide with periods of low insect activity, presumably during the peak of the dry season (36). Based on this hypothesis, however, we could not explain the EVI interannual variability observed in this study.

Finally, our results may be related in part to the sample size and the quality of PAR data used in the spatial–temporal analysis. Although we used the best available data set, only 40 meteorological stations were available for assessing significance in the densely forested parts of the Basin (mostly concentrated in the western Amazon). As a result, we could not test further the effects of PAR on the interannual variability of EVI nor the hypothesis of increased GPP during dry periods with increased PAR.

We thus hypothesize that the apparently conflicting observations of Phillips et al. (19) and Saleska et al. (20) regarding the drought event of 2005 were related to several mechanisms operating simultaneously. GPP (expressed as EVI) appears to have increased because of the production of new leaves and increased PAR (20), whereas aboveground net primary productivity (ANPP) measured in the field concurrently decreased (19) because of higher tree mortality and increased respiration associated with lower PAW and high temperatures. Moreover, the allocation of nonstructural carbohydrates to belowground processes may have increased, given that GPP was higher and ANPP lower during the drought of 2005.

Although we observed important oscillations in weather over the Amazon from 1996–2005 (e.g., a 5.3-mm y^{-1} reduction in PPT), these oscillations were not clearly related to EVI interannual variability in densely forested areas at the Basin scale. Thus, there is a need for additional analyses that couple field measurements with satellite observations to clarify how the Amazon region responds to drought, how those responses will be expressed in the future under increasing drought conditions, and to what extent those responses are captured in satellite observations of canopy photosynthesis.

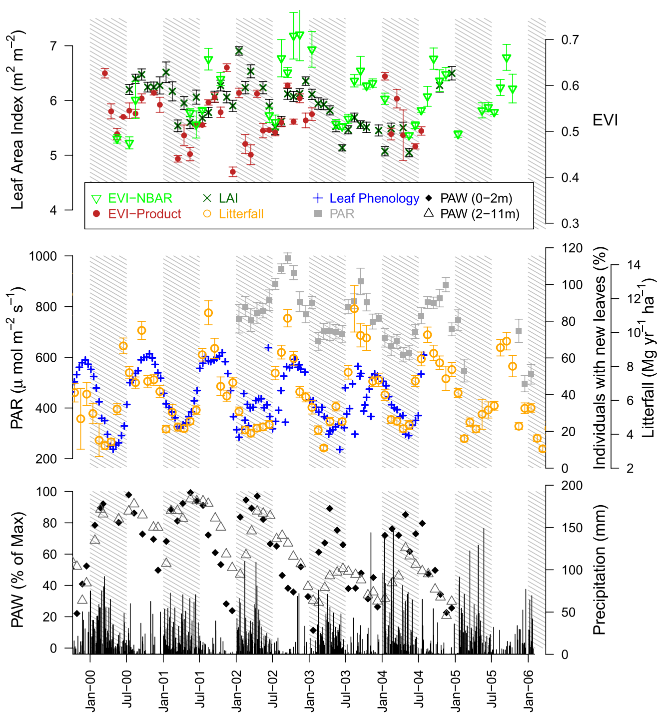

Fig. 4. Temporal patterns of environmental and biophysical correlates of EVI. (*Top*) EVI derived from MODIS NBAR. EVI derived from the collection 5 MODIS product screened to include only good- or best-quality control flags and LAI (*Methods*). (*Middle*) Monthly PAR and bimonthly litterfall and new leaf production (*Methods*). (*Bottom*) PAW (% of maximum) at two depths (0–2 m and 2–11 m) and daily precipitation (in mm).

Methods

MODIS Data. We computed the EVI at a spatial resolution of 500 m from the MCD43A4 (collection 5) NBAR (Nadir Bidirectional Reflectance Distribution Function adjusted reflectance). The NBAR data were standardized to a nadir-view geometry and solar angle and were processed to limit the influence of cloud cover, thereby limiting the influence of seasonal variations in acquisition conditions (30). We further screened the NBAR reflectance quality by using the quality-assurance flags provided for the NBAR product, and we generated a monthly and seasonal composite of "best quality" reflectance [reflectance derived only from full or magnitude inversion (30)] to calculate the EVI. Because of the high number of observations influenced by cloud cover and atmospheric contamination during the wet seasons of 2000–2008, we focused our Basin-wide analysis on the average of the driest months of the year, July–September (referred to as "dry-season EVI"; Fig. S5), thus allowing direct comparisons with Saleska et al. (20). If the EVI in one of these 3 mo was missing, the dry-season average EVI was based on the average of the other 2 mo. If EVI was missing for 2 mo, the dry-season EVI was based on a single value. The NBAR EVI used in this study requires a minimum of three good looks every 16 d (which typically occurs only in the dry season), whereas for the standard EVI product a single good clear day every 16 d is sufficient. As a result, the NBAR-EVI is a less noisy (temporally variable) data set. This procedure thereby assured the largest number of observations of the highest possible data quality. Because we found that the choice of months could influence the spatial patterns of EVI from north to south of the Basin (*SI Text* and Fig. S6), we did not focus our analysis on geographical gradients. Also, we included longitude and latitude as covariates in all statistical analysis (more details are provided in the later discussion of statistical analysis).

EVI Surrounding Meteorological Stations. To compare EVI with in situ climatic measurements, we averaged the EVI data over an area of 8 km × 8 km (256 pixels) surrounding each meteorological station. Then we estimated canopy cover of the vegetation surrounding these meteorological stations as of 2005 (37). This analysis included areas of low (<70%) and high (>70%) canopy cover. The former areas include a mixture of vegetation types. In contrast, densely forested areas included only cells with canopy cover ≥70%. Of the 40 meteorological stations in densely forested areas, 27 had a dry season.

Site-Specific Analysis. The credibility of MODIS-EVI in capturing vegetation dynamics was tested in the Tapajos National Forest, Para, Brazil (2.897°S, 54.952°W) (km-67) using data from both a 1-ha plot (a "control plot" for a rainfall exclusion experiment; details are given in ref. 38) and from an eddy covariance flux tower (16). First, volumetric soil water content was measured each month from 2000–2004 (63 mo) using a series of paired time domain reflectrometry probes situated in five soil pits in the 1-ha plot and converted to PAW (38) for two depths: 0–2 m (PAW-2m); and 2–11 m (PAW-11m). Second, LAI was measured monthly from January 2000 to December 2005 (46 mo) at 100 grid points systematically distributed in the 1-ha control-plot. We used two LiCor 2000 Plant Canopy Analyzers in differential mode (LI-COR 1992). Third, from January 2000 to December 2005 (84 mo), litterfall was collected every 15 d using 100 screened traps (0.5 m^2 each) located in the LAI grid points. Fourth, visual assessments of the presence of new foliage were conducted monthly between August 1999 and August 2004 (60 mo) for all individuals ≥10 cm in diameter at breast height in the 1-ha plot (480 individuals). Here we present the percent of individuals with new leaves at a given census. Finally, PAR was measured from 2002–2006 (40 mo) using a LiCor 190-SA at a height of 63.6 m (16). At this site, annual precipitation ranges from 1,700–3,000 mm, and during the dry season rainfall rarely exceeds 75 mm mo^{-1}. There were 39 mo with observations for the C5 EVI product and 37 mo with observations for EVI NBAR.

NBAR-EVI and EVI product. For the site-specific analysis, we used both the EVI derived from the NBAR product (500-m resolution) and the standard EVI product (collection 5) composited each 16 d, with a spatial resolution of 250 m × 250 m. As noted earlier, the NBAR-EVI data limit the attenuating effects of the atmosphere and viewing conditions (30) but require temporal compositing to maximize data quality. We screened the NBAR reflectance quality using the quality-assurance flags provided for the NBAR product, generating a monthly and seasonal composite of "best quality" reflectance (30). The MODIS standard **EVI** product also was screened based on the MODIS product quality flags (e.g., reliability). No corrections for solar or viewing conditions are made in the standard EVI product. Thus, differences between the NBAR-EVI and standard EVI products could be related to the MODIS Bidirectional Reflectance Distribution Function model used to solve for surface reflectance, to procedures used to screen for cloud contamination and the normalization for solar illumination angle, or to all such factors. Moreover, we compared EVI through repeated measurements of individual pixels; thus corrections for the influences of viewing conditions and solar angle were potentially quite important.

Climate. Monthly data from ~280 meteorological stations (5) were used to derive dry- and wet-season averages for the Amazon from 1996–2005) (Fig. 1*A*). In the locations where meteorological stations were available, solar radiation was derived from the VIS Meteosat channel from the satellite GOES-8, following a physical model based on the heat transfer equation (details are given in ref. 39). Solar radiation was divided into infrared and visible (400–700 nm) bands; we used the latter (referred as "PAR") in our analysis. In testing the quality of modeled PAR, we found that it showed a positive and relatively weak relationship with PAR (R^2 = 31%) and NBAR EVI measured at the Tapajos site (R^2 = 32%). Next we assessed seasonal averages of climatic variables over time for each meteorological station, using a linear mixture model that accounted for spatial and temporal autocorrelation (i.e., random effects of space and time) and a parameter to attenuate the effects of dry years (i.e., 1998 and 2005). Finally, the slopes of these regressions were tested for differences against the null model of zero change over time (40), which included only random effects. For each of the 280 meteorological stations, we calculated the categorical variable PPT history (i.e., the average dry-season precipitation based on data from 1996 through 2005).

Statistical Analysis of EVI and Climatic Variables. ***Basin-wide (mixed vegetation types).*** A general linear model (*M1*) of EVI in areas of mixed vegetation (i.e., not only in densely forested areas) comprised three components: (*i*) the continuous predictor variables VPD, PAR, PPT, canopy cover (CC), and the interaction of CC with the other covariates; (*ii*) error terms assumed to be spatially autocorrelated according to an exponential spatial structure; and (*iii*) covariates of longitude and latitude, to capture the large-scale spatial gradient of EVI. We fitted this model to the data for each year of the study (2000–2005) and therefore do not account for interannual variability in mixed vegetation areas; that calculation is complex because of land use change over time. The model does allow for separate regression coefficients and autocorrelation coefficients for each year.

Densely forested areas. Our general linear statistical models (*M2*) of EVI in forested areas comprised three components. First, covariates of PAR, VPD, and PPT (each term interacted with PPT history class, a categorical variable) were included to assess the effects of climate on EVI in three different climatic regions: seasonally very dry regions (PPT history class: 0–65 mm), seasonally dry regions (PPT history class: 66–100 mm), and nonseasonal regions (PPT history class: >100 mm). Second, longitude and latitude were included as covariates to capture the large-scale spatial gradient of EVI. Third, the error terms were assumed to have an autoregressive correlation structure of order 1 (40) to account for temporal autocorrelation among observations from the same locations over several years. Note that for forested areas we did not find evidence of spatial autocorrelation in the residuals from the fitted model.

Hierarchical partitioning. In both mixed vegetation and densely forested areas, we used hierarchical partitioning (23) as a complementary statistical method to evaluate each covariate's contribution to EVI. In this method, the variance in the response variable (EVI) shared by two predictors can be partitioned into the variance of EVI uniquely attributable to each predictor. For mixed-vegetation areas, for each year of the study, we used hierarchical partitioning to evaluate model 1 (*M1*), but without a spatial structure. For densely forested areas, we evaluated a model that included all climatic variables, the location of each meteorological station, longitude, latitude, and year; this model is referred to throughout as a "variation of *M2*." Because PPT was dependent on location of the meteorological station, we did not include this variable in the hierarchical partitioning analysis.

Relationship of the Variability of EVI with PAW. We first calculated for each MODIS pixel the coefficient of variation of the EVI for the period 2000–2008, but we retained only pixels with ≥70% of canopy cover and with data for ≥6 y. The Amazon Basin then was stratified by PAW from 0–10 m in depth (class 1: 470–985 mm; class 2: 986–1,280 mm; class 3: 1,281–1,500 mm; class 4: 1,500–2,100 mm) (see ref. 5 for the calculation of PAW). Finally, the coefficient of variation of the EVI between the four PAW classes was compared visually.

ACKNOWLEDGMENTS. We thank the Brazilian Institute of Environment and Renewable Natural Resources for providing access to the Floresta Nacional do Tapajos, the crew from the Instituto de Pesquisa Ambiental da Amazônia and Embrapa for their help with data collection and analysis, P. Lefebvre [Woods Hole Research Center (WHRC)] for assistance with the PAW maps, and L. Hutyra (Boston University) for Tapajos PAR data. The manuscript was improved by constructive comments of F. E. Putz [University of Florida (UFL)] and M. Slot (UFL), by discussions with B. Bolker (UFL), M. Coe (WHRC), A. Shenkin (UFL), F. Belshe, and the participants in the Ecosystem Ecology class at the University of Florida, and by the thoughtful, careful comments of the anonymous reviewers. We appreciate the financial support from the National Science Foundation, the National Aeronautics and Space Administration, the large-scale Biosphere-Atmosphere Experiment in Amazonia, the United States Agency for International Development, the National Council for Scientific and Technological Development, and the Gordon and Betty Moore Foundation. P.M.B. received support from Coordination for Improvement of Higher Education Personnel-Fulbright for dissertation research.

1. Malhi Y, et al. (2008) Climate change, deforestation, and the fate of the Amazon. *Science* 319:169–172.
2. Costa MH, Foley JA (2000) Combined effects of deforestation and doubled atmospheric CO2 concentrations on the climate of Amazonia. *J Clim* 13:18–34.
3. Werth D, Avissar R (2002) The local and global effects of Amazon deforestation. *J Geophys Res* 107:8087–8095.
4. Nobre CA, Sellers PJ, Shukla J (1991) Amazonian deforestation and regional climate change. *J Clim* 4:957–988.
5. Nepstad D, et al. (2004) Amazon drought and its implications for forest flammability and tree growth: A basin-wide analysis. *Glob Change Biol* 10:704–717.
6. Cox PM, et al. (2008) Increasing risk of Amazonian drought due to decreasing aerosol pollution. *Nature* 453:212–215.
7. Marengo JA, et al. (2008) The drought of Amazonia in 2005. *J Clim* 21:495–516.
8. Nepstad DC, Stickler CM, Filho BS, Merry F (2008) Interactions among Amazon land use, forests and climate: Prospects for a near-term forest tipping point. *Philos Trans R Soc Lond B Biol Sci* 363:1737–1746.
9. Fisher RA, Williams M, Do Vale RL, Da Costa AL, Meir P (2006) Evidence from Amazonian forests is consistent with isohydric control of leaf water potential. *Plant Cell Environ* 29:151–165.
10. Betts R, Sanderson M, Woodward S (2008) Effects of large-scale Amazon forest degradation on climate and air quality through fluxes of carbon dioxide, water, energy, mineral dust and isoprene. *Philos Trans R Soc Lond B Biol Sci* 363:1873–1880.
11. Huntingford C, et al. (2008) Towards quantifying uncertainty in predictions of Amazon 'dieback'. *Philos Trans R Soc Lond B Biol Sci* 363:1857–1864.
12. Mayle FE, Power MJ (2008) Impact of a drier Early-Mid-Holocene climate upon Amazonian forests. *Philos Trans R Soc Lond B Biol Sci* 363:1829–1838.
13. Lloyd J, Farquhar GD (2008) Effects of rising temperatures and [CO2] on the physiology of tropical forest trees. *Philos Trans R Soc Lond B Biol Sci* 363:1811–1817.
14. Graham EA, Mulkey SS, Kitajima K, Phillips NG, Wright SJ (2003) Cloud cover limits net CO2 uptake and growth of a rainforest tree during tropical rainy seasons. *Proc Natl Acad Sci USA* 100:572–576.
15. Saleska SR, et al. (2003) Carbon in Amazon forests: unexpected seasonal fluxes and disturbance-induced losses. *Science* 302:1554–1557.
16. Hutyra LR, et al. (2007) Seasonal controls on the exchange of carbon and water in an Amazonian rain forest. *J Geophys Res* 112: G04099.
17. Meir P, et al. (2009) The effects of drought on Amazonian rainforests. *Geophys Monogr Ser*, pp 429–459, 10.1029/2008GM000882.
18. Oliveira RS, Dawson TE, Burgess SSO, Nepstad DC (2005) Hydraulic redistribution in three Amazonian trees. *Oecologia* 145:354–363.
19. Phillips OL, et al. (2009) Drought sensitivity of the Amazon rainforest. *Science* 323: 1344–1347.
20. Saleska SR, Didan K, Huete AR, da Rocha HR (2007) Amazon forests green-up during 2005 drought. *Science* 318:612.
21. Huete A, et al. (2002) Overview of the radiometric and biophysical performance of the MODIS vegetation indices. *Remote Sensing of Environment* 83:195–213.
22. Samanta A, et al. (2010) Amazon forests did not green-up during the 2005 drought. *Geophys Res Lett* 37:L05401–L05406.
23. Murray K, Conner MM (2009) Methods to quantify variable importance: Implications for the analysis of noisy ecological data. *Ecology* 90:348–355.
24. Wright SJ, Carrasco C, Calderon O, Paton S (1999) The El Nino Southern Oscillation, variable fruit production, and famine in a tropical forest. *Ecology* 80: 1632–1647.
25. Brando PM, et al. (2008) Drought effects on litterfall, wood production and belowground carbon cycling in an Amazon forest: Results of a throughfall reduction experiment. *Philos Trans R Soc Lond B Biol Sci* 363:1839–1848.
26. Nepstad DC, Tohver IM, Ray D, Moutinho P, Cardinot G (2007) Mortality of large trees and lianas following experimental drought in an Amazon forest. *Ecology* 88: 2259–2269.
27. Myneni RB, et al. (2007) Large seasonal swings in leaf area of Amazon rainforests. *Proc Natl Acad Sci USA* 104:4820–4823.
28. Huete AR, et al. (2006) Amazon rainforests green-up with sunlight in dry season. *Geophys Res Lett* 33:L06405–L06405.
29. Xiao X, et al. (2005) Satellite-based modeling of gross primary production in a seasonally moist tropical evergreen forest. *Remote Sensing of Environment* 94:105–122.
30. Schaaf CB, et al. (2002) First operational BRDF, albedo nadir reflectance products from MODIS. *Remote Sens Environ* 83:135–148.
31. Nepstad DC, et al. (1994) The role of deep roots in the hydrological and carbon cycles of Amazonian forests and pastures. PhD thesis. (Yale Univ, New Haven, CT).
32. Goetz SJ, Prince SD (1999) Modelling terrestrial carbon exchange and storage: Evidence and implications of functional convergence in light-use efficiency. *Advances in Ecological Research* 28:57–92.
33. Doughty CE, Goulden ML (2008) Seasonal patterns of tropical forest leaf area index and CO2 exchange. *J Geophys Res* 113:G00B06–G00B18.
34. Wright SJ, van Schaik CP (1994) Light and the phenology of tropical trees. *Am Nat* 143:192–199.
35. Rivera G, et al. (2002) Increasing day-length induces spring flushing of tropical dry forest trees in the absence of rain. *Trees - Structure and Function* 16:445–456.
36. Aide TM (1993) Patterns of leaf development and herbivory in a tropical understory community. *Ecology* 74:455–466.
37. Hansen MC, et al. (2003) Global percent tree cover at a spatial resolution of 500 meters: First results of the MODIS vegetation continuous fields algorithm. *Earth Interactions* 7:1–15.
38. Nepstad DC, et al. (2002) The effects of partial throughfall exclusion on canopy processes, aboveground production, and biogeochemistry of an Amazon forest. *J Geophys Res* 107:8085–8103.
39. Ceballos JC, Moura GBA (1997) Solar radiation assessment using Meteosat 4-VIS imagery. *Solar Energy* 60:209–219.
40. Baayen H (2008) *Analyzing Linguistic Data: A Practical Introduction to Statistics Using R* (Cambridge Univ Press, Cambridge, UK).